Organic Electronics 37 (2016) 197–206

Contents lists available at ScienceDirect

Organic Electronics

journal homepage: www.elsevier.com/locate/orgel

A highly flexible solid-state supercapacitor based on the carbon nanotube doped graphene oxide/polypyrrole composites with superior electrochemical performances

Haihan Zhou*, Hua-Jin Zhai**

Institute of Molecular Science, Key Laboratory of Materials for Energy Conversion and Storage of Shanxi Province, Key Laboratory of Chemical Biology and Molecular Engineering of Education Ministry, Shanxi University, Taiyuan, 030006, China

ARTICLE INFO

Article history:
Received 17 March 2016
Received in revised form
10 May 2016
Accepted 28 June 2016
Available online 5 July 2016

Keywords:
Supercapacitor
Conducting polymers
Graphene oxide
Carbon nanotubes
Composites

ABSTRACT

Flexible electrodes of ternary composites, in which highly conductive carbon nanotube films (CNFs) are coated with carbon nanotube-doped graphene oxide/polypyrrole (CNT-GO/PPy), have been fabricated via facile electrochemical synthesis. Long and short CNTs are separately doped into the composites (lCNT-GO/PPy and sCNT-GO/PPy) and their electrochemical performances are compared. Electrochemical measurements indicate that the doping of CNTs in the composites significantly improves the electrochemical behaviors of the GO/PPy electrodes. Notably, the lCNT-GO/PPy electrodes show superior electrochemical properties with respect to the sCNT-GO/PPy electrodes, which is related to the introduction of abundant CNTs in the former electrodes and their special microstructures. Two symmetric electrodes with the lCNT-GO/PPy composites coated on CNFs are assembled to fabricate a solid-state supercapacitor device, which features lightweight, ultrathinness, and high flexibility. The device achieves a high areal and volumetric specific capacitance of 70.0 mF cm^{-2} at 10 mV s^{-1} and 6.3 F cm^{-3} at 0.043 A cm^{-3}, respectively. It also shows superior rate performance and cycle stability, with a capacitance retention rate of 87.7% for 10,000 cycles. The supercapacitor device fabricated is promising for the use in lightweight and flexible integrated electronics.

1. Introduction

Currently there has been tremendous interest in the development of flexible, lightweight, and thin energy storage devices, which primarily aims for promising applications in flexible/portable electronics such as wearable devices, flexible photovoltaic cells, and rollable displays [1–3]. Flexible supercapacitors as one kind of energy storage device can meet the increasing demands in flexible/portable electronics, due to their large power density, moderate energy density, long cycle life, and operational safety [4,5]. Depending on the charge-storage mechanism, supercapacitors can be categorized into electrical double-layer capacitors (EDLC) and pseudocapacitors. EDLCs store charges at the electrode/electrolyte interface and typically use carbonaceous materials with high surface areas. Pseudocapacitors, which rely on fast and reversible Faradaic redox reactions at the surface or near-surface of the electroactive species, employ materials such as conducting polymers and transition metal oxides/hydroxide [6–8].

As is well known, electrode material is one of the crucial factors that influence the performance of the supercapacitors. Electrode materials based on different charge-storage mechanisms have been extensively studied for supercapacitor applications. However, each kind of materials has its limitation for electrochemical energy storage. In general, carbonaceous materials, which store energy by the electrical double-layers, show fast charge-discharge and long cycle life, but these have limited specific capacitance. On the other hand, transition metal oxides and conducting polymers have high energy density, but yet they suffer from a drawback of poor conductivity and low cycle life [9,10]. Thus, considerable recent effort has been devoted to synthesizing hybrid materials for electrodes, such as TiO_2@polyaniline core-shell nanowires [11], $NiCo_2O_4$@polypyrrole coaxial nanowire arrays [12], and MnO_2@polyaniline composites [13]. These composite materials combine the advantages of both EDLCs and pseudocapacitors and strive to meet the demand of large energy density, high power density, and long-

* Corresponding author.
** Corresponding author.
E-mail addresses: hhzhou@sxu.edu.cn (H. Zhou), hj.zhai@sxu.edu.cn (H.-J. Zhai).

http://dx.doi.org/10.1016/j.orgel.2016.06.036
1566-1199/

term cycle life.

Conducting polymers (CPs) exhibit high Faradaic pseudocapacitance, which makes them promising for supercapacitor applications. To further improve their properties as electrode materials (including capacitance, conductivity, stability, and mechanical strength), CPs have been prepared in the form of composites with other materials such as MnO_2 [14], surfactant [15], and carbon nanomaterials [16]. In consideration of scalability and cost, graphene oxide (GO) has become increasingly important as it can be easily fabricated from natural graphite. GO has a negative surface charge due to the abundant oxygen containing functional groups, so it can form stable dispersions in water [17]. Moreover, the GO sheets exhibit a large specific surface area. Recently, a number of studies have been carried out to synthesis the GO/CPs composites for high-performance supercapacitors. For instance, Li et al. prepared graphene oxide/polypyrrole (GO/PPy) nanowires via in-situ chemical polymerization [18]. Cao et al. fabricated three dimensional (3D) GO/PPy composite electrodes through electrochemical deposition [19]. Wu et al. reported a facile synthesis of GO/CPs composites, in which CPs represents polyaniline (PANI) and PPy, using in situ oxidative polymerization [20]. In addition, GO/PPy composite electrodes have also been prepared by electrochemical deposition in our previous work [21].

However, the capacitive performance of the GO/CPs composites is still hindered as a result of the insulating nature of GO (conductivity: 1.28×10^{-9} S cm^{-1}) in the composites [19]. To this end, studies were carried out to prepare the reduced graphene oxide/CPs composites through further reduction of GO [22–26]. However, the further reduction adds to the complexity of electrode preparation, and the capacitive performances of obtained rGO/CPs electrodes were not much improved. Carbon nanotubes (CNTs) have been widely utilized as the electrode materials for supercapacitor, owing to their high conductivity, ideal specific surface area, low specific weight, and chemical stability [27]. Furthermore, carboxylated CNTs can act as the counter-ions, which are readily doped into the composites during polymerization of CPs. As one of the most studied conducting polymers, PPy features high electrical conductivity, large specific capacitance, chemical stability, and low cost [28]. Thus, this study is devoted to improving the electrochemical performances of GO/PPy by doping CNTs via one-pot electrochemical polymerization, during which the anionic GO sheets and carboxylated CNTs serve simultaneously as the counter-ions doped into the composites. In particular, the effect of two types of CNTs (short versus long) are investigated and compared in terms of improving the electrochemical performances of the GO/PPy composites.

One critical factor in fabricating flexible supercapacitors is to develop the high performance flexible electrodes. A routine method to make flexible electrodes is loading electroactive species on the flexible substrates with porous structures. Despite their high flexibility and ion accessibility, the electrical conductivity of such electrodes is limited by the insulate substrates like non-woven fabrics, cellulose papers, and porous cotton, which affect the capacitive performances of the supercapacitors fabricated. Moreover, the total weight of the device also increases due to the use of insulate substrates, leading to the decrease of capacitance per unit weight [29]. Carbon nanotube films (CNFs) feature lightweight, ultrathinness, superior flexibility, high electrical conductivity, and favorable mechanical strength, and thus they are suitable substrates for flexible electric devices [30].

In the present work, in order to obtain the highly flexible, lightweight, and ultrathin electrodes for supercapacitors, we choose CNFs as the electrode substrates as well as the current collector. The CNFs, loaded with ternary composites of short and long CNT doped GO/PPy (sCNT-GO/PPy and lCNT-GO/PPy), are prepared as electrodes via one-pot electrochemical polymerization. Electrochemical characterizations including cyclic voltammetry (CV), galvanostatic charge/discharge (GCD) measurements, and electrochemical impedance spectroscopy (EIS) were performed to compare their electrochemical behaviors. To testify the feasibility of the CNFs based composite electrodes for use as flexible supercapacitor devices, a solid-state supercapacitor was fabricated by assembling two symmetric lCNT-GO/PPy composite coated CNFs electrodes with PVA-H_3PO_4 gel as a solid electrolyte. Its capacitive performances and cycle stability were tested and a three-supercapacitor tandem device successfully lit a light-emitting diode (LED). The latter observation should stimulate potential practical applications of such flexible supercapacitor.

2. Experimental section

2.1. Materials

Pyrrole (99%) was obtained from Aladdin Chemistry Co., Ltd. Natural graphite powder (325 mesh) was purchased from Tianjin Guangfu Research Institute. Long and short carboxylated multi-wall carbon nanotubes (lCNT-COOH and sCNT-COOH) were purchased from Chengdu Organic Chemicals Co., Ltd. Their length is 10–30 and 0.5–2 μm, respectively, and the outer diameter for both of them is < 8 nm, which are made by chemical vapor deposition (CVD). Carbon nanotube thin films (CNFs, thickness of 20 μm) were supplied by Soochow Hengqiu Tech. Inc. Polyvinyl alcohol (PVA)-124 were purchased from Sinopharm Chemical Reagent Co., Ltd.

2.2. Fabrication of the electrodes and the supercapacitor assembly

The flexible electrodes were fabricated through one-pot electrochemical polymerization of the CNT-GO/PPy composites on the CNFs substrate. The aqueous bath for electrochemical polymerization consists of 0.2 M pyrrole monomer, 1 mg mL^{-1} GO, and 1 mg mL^{-1} CNT-COOH (long or short) without any supporting electrolyte, which were dispersed adequately under ultrasonication for about 15 min before use. Thereinto, GO was prepared from natural graphite powder with the modified Hummers method and from subsequent exfoliation by ultrasonication [31,32]. Electropolymerization was performed with a constant low current density of 1 mA cm^{-2} for 30 min in a three-electrode cell, in which CNFs (1 cm × 1 cm of conductive areas) act as the working electrode, a Pt foil with large area serves as the counter electrode, and a saturated calomel electrode (SCE) as the reference electrode. After that, the composite films coated CNFs electrodes were rinsed with deionized water to remove monomer and oligomer residues. The obtained flexible long and short CNT doped GO/PPy composite electrodes are denoted as lCNT-GO/PPy and sCNT-GO/PPy electrodes, respectively. For comparison, the GO/PPy electrodes were prepared with the same electropolymerization procedure in the carboxylated CNT-free aqueous bath. During the electropolymerization, a constant charge density of 1.8 C cm^{-2} passed for the composite electrodes.

The flexible solid-state supercapacitor was assembled with two pieces of symmetric composites coated CNF electrodes, with a separator (filter paper with 20 μm thickness) sandwiched in between. PVA-H_3PO_4 gel was used as the solid electrolyte. Subsequently the device was placed in atmosphere at room temperature to vaporize the excess water. The PVA-H_3PO_4 gel electrolyte was simply prepared as follows: 1 g of concentrated H_3PO_4 was mixed with 10 mL of deionized water and then 1 g of PVA powder was added. The mixture was heated to 85 °C under vigorous stirring until the solution became clear. The gel electrolyte was obtained after cooling the solution down.

2.3. Characterizations

The FT-IR spectra were obtained with a Bruker Tensor 27 FT-IR Spectrometer, and the tested samples were prepared by potassium bromide tabletting. A field emission scan electron microscope (SEM, JSM-6701F, JEOL) and a high resolution transmission electron microscope (TEM, JEM-2100, JEOL) were used to observe the morphology of as-prepared composites. The samples for tests were scraped from the composite films coated conducting glasses for the FT-IR and TEM characterizations, because it is difficult to scrape the films directly from the surface of CNFs.

2.4. Electrochemical measurements

The electrochemical behaviors of as-prepared electrodes were recorded with two-electrode cell, which consists of two pieces of identical composite coated CNF electrodes (one oxidized and one reduced), with a sandwiched filter paper soaked with 1.0 M KCl electrolyte as the separator. The CV, GCD, and EIS measurements were carried out with a CHI 660E electrochemical workstation (Chenhua, China). The CV and GCD curves were tested between potentials of −0.5 to 0.5 V at various scan rates and current densities. The EIS were recorded using 5 mV (rms) AC sinusoid signal and at a frequency range from 10^5 to 0.01 Hz at the open circuit potential.

3. Results and discussion

3.1. Composition and morphology

In the one-pot electrochemical oxidative polymerization, the polymerization of pyrrole monomer takes place, during which carboxylated CNTs and anionic GO act simultaneously as the charge carriers in the solution as well as the counter ions for charge balancing of PPy. Consequently, the CNT-GO/PPy composites form. The FT-IR characterization was performed to confirm the formation of the sCNT-GO/PPy and lCNT-GO/PPy composites. The obtained FT-IR spectra are shown in Fig. 1. In the spectrum of GO, the peak at 1055 cm^{-1} is characteristic of the epoxide group, the peaks located at 1413 and 1235 cm^{-1} originate from the O—H deformation and C—OH stretching vibration, and the peak at 1703 cm^{-1} is related to the C═O stretching of carbonyl [33]. The peak at 1722 cm^{-1} in the sCNT-COOH and lCNT-COOH spectra is due to C═O stretching of the carboxyl [34], indicating the anionic nature of GO and CNT-COOH.

The peaks at 1540 and 1457 cm^{-1} in the PPy spectrum are caused by the stretching vibration of C—C and C—N in the pyrrole ring, respectively [35,36]. The characteristic peaks of PPy at 1546 and 1460 cm^{-1} appear in the sCNT-GO/PPy and lCNT-GO/PPy composites, demonstrating the presence of PPy in the composites. Furthermore, the peak at 1038 cm^{-1}, attributed to the C—H in-plane vibration of PPy ring, has shifted to 1033 cm^{-1} for the two types of composites. The shift is related to the electrostatic interaction originated from the PPy cations and the anions of GO and CNT-COOH. It should be noted that the bands for GO and CNT-COOH are detected scarcely for the composites, probably because these are too weak or overlapped with the peaks of PPy.

The morphology of as-prepared composites is critical to affect their electrochemical properties. In this investigation, the mass of the GO/PPy, lCNT-GO/PPy, and sCNT-GO/PPy composites deposited on the CNF substrates is 1.10, 0.97, and 0.98 mg, respectively, and their representative SEM images are depicted in Fig. 2. It can be seen from the GO/PPy images (Fig. 2 (a) and 2 (b)) that a curly and wrinkled morphology of GO nanosheets is observed. The two-dimensional nanosheets interconnect with each other, indicating that GO dominates the GO/PPy composites.

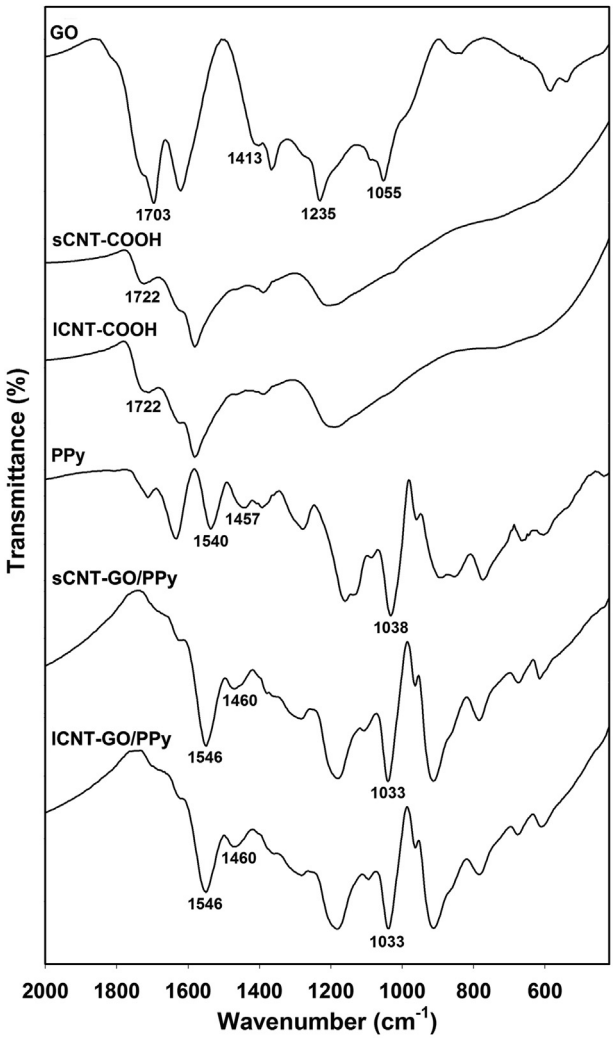

Fig. 1. FT-IR spectra of GO, sCNT-COOH, lCNT-COOH, PPy, sCNT-GO/PPy, and lCNT-GO/PPy composites.

However, after the CNTs are doped into the composites, the lCNT-GO/PPy and sCNT-GO/PPy composites have very different morphology. Notably, the curly sheet-like GO largely disappears. This can be attributed to the enhanced polymerization of PPy upon the introduction of CNTs, which coats the GO and covers its morphology. The enhanced polymerized PPy should facilitate the increase of Faradaic pseudocapacitance of the composites. Moreover, it can be obviously observed from the images at high magnification (Fig. 2(d) and (f)) that only a small amount of CNTs scatter in the sCNT-GO/PPy composites (marked with red arrows), which is probably because these CNTs are too short to construct an interconnected network. However, in lCNT-GO/PPy, relatively more CNTs are introduced within the composites. These long CNTs across the composites form an interconnected conductive nano-network (marked with red arrows). The large amount of anionic CNTs introduced into the composites can make them less compact, consequently facilitating ion diffusion within the composites.

TEM characterization was conducted to further examine the microstructure of the composites. It can be seen from Fig. 3 that PPy-coated CNTs load on GO sheets in the two types of CNT-GO/PPy composites, indicating that during the electropolymerization GO not only serves as the counter-ion, but also as the substrate to load the PPy-coated CNTs. However, for sCNT-GO/PPy only a small

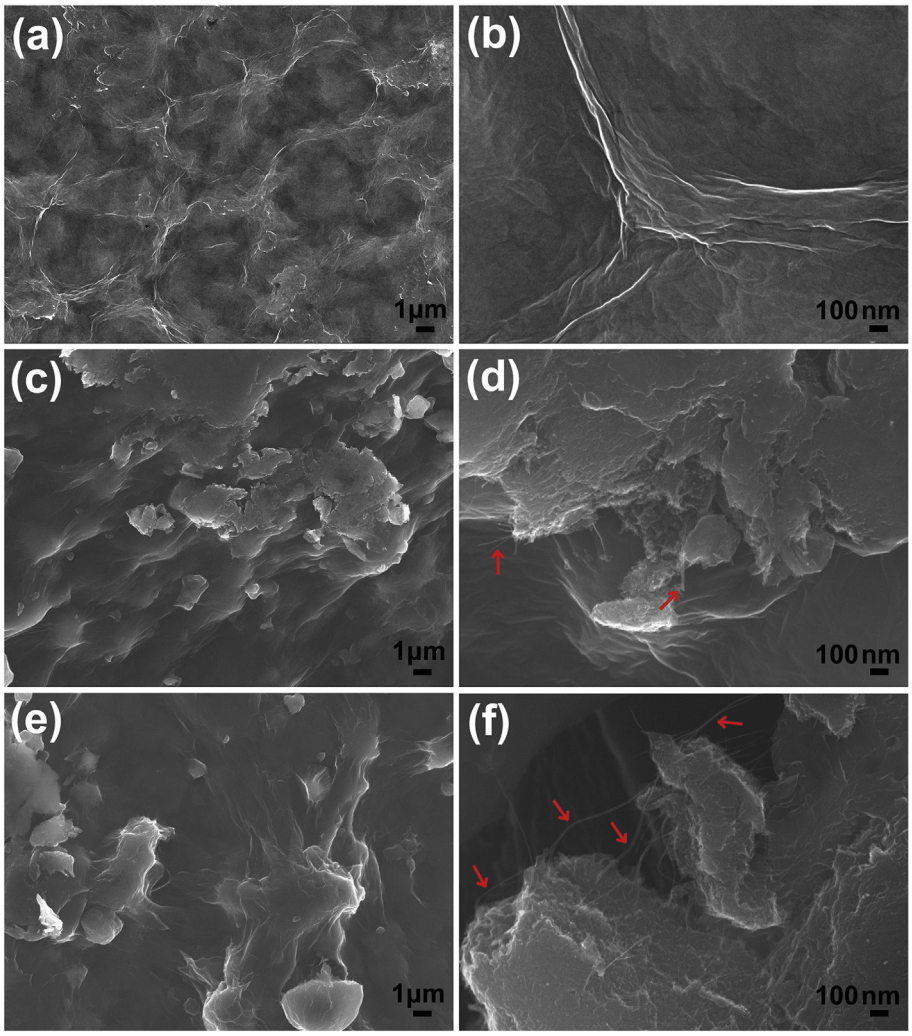

Fig. 2. Representative SEM images of GO/PPy (a, b), sCNT-GO/PPy (c, d), and lCNT-GO/PPy (e, f) composites at low (left column) and high (right column) magnification. Representative CNTs doped in the composites are marked with red arrows. (For interpretation of the references to colour in this figure legend, the reader is referred to the web version of this article.)

amount of CNTs are shown, whereas for lCNT-GO/PPy a relatively large amount of CNTs are doped. This observation further indicates that relatively more CNTs are introduced into the lCNT-GO/PPy composites and they are interconnected. In short, the TEM results are in line with those of SEM. The morphology of the composites indicates that relatively more CNTs are doped into lCNT-GO/PPy. Meanwhile these long CNTs form an interconnected, conductive nano-network within the composites.

3.2. Electrochemical performances of the flexible composite electrodes

For ternary CNT-GO/PPy composites, PPy can provide large Faradaic pseudocapacitance, GO sheets and CNTs have large specific surface area and contribute to high electric double layer capacitance, whereas the doped CNTs with high conductivity help make up the disadvantage of insulating GO for high-efficiency charge transfer. To investigate the influence of doped long and short CNTs on the electrochemical properties of the CNT-GO/PPy composites, electrochemical measurements including CV, GCD, and EIS were carried out.

Fig. 4(a) shows the CV curves of the GO/PPy, sCNT-GO/PPy, and lCNT-GO/PPy electrodes at varying scan rates. All curves have the rectangular shape and symmetric I-E responses at 10 mV s^{-1}. Meanwhile, the current obviously increases with the increase of scan rate, showing ideal capacitive behavior. It should be noted that the CV curves at all three scan rates do not reveal obvious redox peaks in the whole CV scan process, which is because the electrochemical measurements were performed with two-electrode system assembled by two pieces of identical electrodes. During the tests, one piece of electrodes was oxidized and the other reduced, resulting in the oxidation/reduction peaks of PPy being unobvious. In this study, the capacitive behaviors were examined with two electrode system, which allows a better estimation of materials performance for electrochemical capacitors [37]. In addition, areal specific capacitance is a better indicator than gravimetric specific capacitance for supercapacitor performance with the purpose of applications for small scale electronics and stationary energy storage devices [38], so the specific capacitance of electrodes was calculated in area units in this study.

Based on the CV curves, the areal specific capacitance (Cs) of electrodes is obtained according to the following equation:

$$C_S = \left(\int idV\right) \Big/ (S \times \Delta V \times v) \tag{1}$$

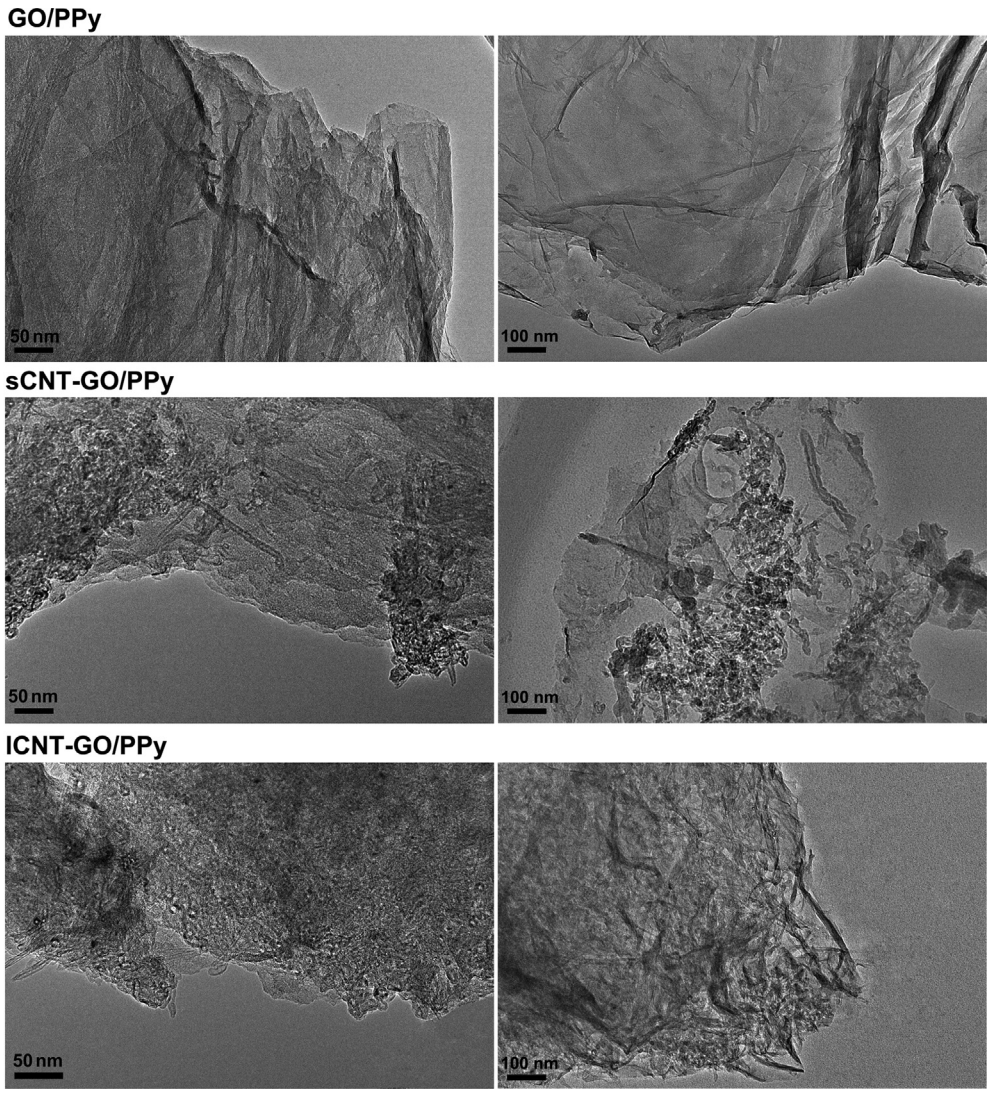

Fig. 3. Representative TEM images of GO/PPy, sCNT-GO/PPy, and lCNT-GO/PPy composites.

where Cs is the areal specific capacitance (F cm^{-2}), $\int$ idV the integrated area of the CV curve, S the surface area of active materials (cm^2; which is 1 cm^2 in this study), ΔV the scanning potential window in V, and v the scan rate (V s^{-1}). It can be seen from Fig. 4(b) that the two types of CNTs doped GO/PPy electrodes deliver the larger specific capacitance at all scan rates with respect to the GO/PPy electrodes, indicating that the capacitive properties of the GO/PPy electrodes are significantly boosted due to the doping of CNTs. Meanwhile, it is also shown that the lCNT-GO/PPy electrodes have slightly higher specific capacitance than the sCNT-GO/PPy electrodes at all the CV scan rates, indicating that the long CNTs can better promote the capacitive performances of the GO/PPy composites.

Thereinto, the areal capacitance of the GO/PPy electrodes is 140.0 mF cm^{-2} at 10 mV s^{-1}, while the sCNT-GO/PPy and lCNT-GO/PPy electrodes reach 183.2 mF cm^{-2} (with an increase of 30.8%) and 202.3 mF cm^{-2} (with an increase of 44.5%) at 10 mV s^{-1}, respectively. The latter values are higher than those of supercapacitor materials reported previously, such as active carbon cloth (88 mF cm^{-2} at 10 mV s^{-1}) [39], CNT/TiO_2/ionomer (88 mF cm^{-2} at 5 mV s^{-1}) [40], TiO_2@PPy nanowires (64.6 mF cm^{-2} at 10 mV s^{-1}) [41], and PANI/graphite oxide composites (25 mF cm^{-2} at 5 mV s^{-1}) [42].

The capacitive performances of the two types of CNT-GO/PPy electrodes were further compared by GCD tests. Fig. 5(a) shows the GCD curves of the lCNT-GO/PPy and sCNT-GO/PPy electrodes at the GCD current density of 0.5 mA cm^{-2}. It can be seen that both types of electrodes exhibit triangle-shaped curves, and the lCNT-GO/PPy electrodes have a longer discharge time than the sCNT-GO/PPy electrodes. Furthermore, the lCNT-GO/PPy electrodes have lower IR drops, demonstrating that the capacitor cells constructed with the lCNT-GO/PPy electrodes have a lower internal resistance. The low internal resistance is of importance for energy-storing devices because less energy will be wasted to produce unwanted heat during the processes of charging/discharging.

The areal specific capacitance of electrodes can be calculated from the GCD curves based on the following equation:

$$C_S = (2 \times i \times t)/(S \times \Delta V) \quad (2)$$

where Cs represents the areal specific capacitance (F cm^{-2}), i the discharge current (A), t the discharge time (s), S the surface area of active materials on the electrode (1 cm^2 in this study), and ΔV the scanning potential window (V). In accordance with the results of CV tests, the lCNT-GO/PPy electrodes show higher specific capacitance over all GCD current densities (Fig. 5(b)). The sCNT-GO/PPy

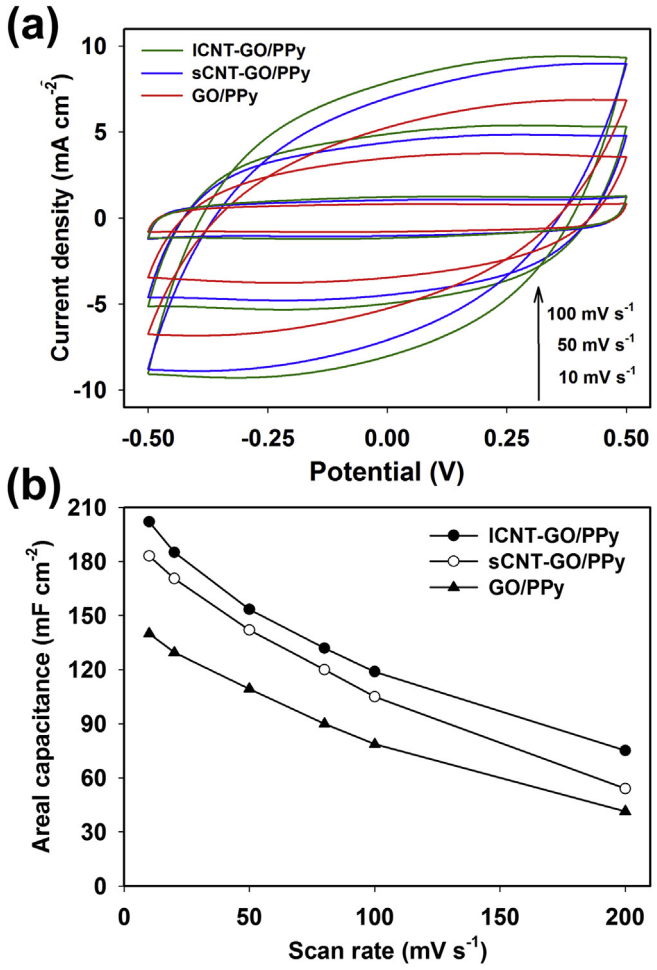

Fig. 4. Cyclic voltammograms at various scan rates (a) and relationship of areal specific capacitance with CV scan rate (b) for GO/PPy, sCNT-GO/PPy, and lCNT-GO/PPy composite electrodes.

electrodes have a specific capacitance of 209.0 mF cm^{-2} at 0.2 mA cm^{-2}, whereas that of the lCNT-GO/PPy electrodes is 227.1 mF cm^{-2} at 0.2 mA cm^{-2}. These values are to be compared with those of the electrode materials previously reported: Fe_3O_4@SnO_2 core-shell nanorod array (7.013 mF cm^{-2} at 0.2 mA cm^{-2}) and 3D porous graphene/PANI composites (67.2 mF cm^{-2} at 0.05 mA cm^{-2}) [43,44].

The EIS is a powerful tool to evaluate the charge transport and ion diffusion at the electrode/electrolyte interface. Fig. 5(c) illustrates the EIS complex plane plots of the lCNT-GO/PPy and sCNT-GO/PPy electrodes. It can be observed that both types of electrodes show a vertical trend for impedance plots at low frequencies, indicative of capacitive character. Comparing with the sCNT-GO/PPy electrodes, the straight line of the lCNT-GO/PPy electrodes at the low frequency leans more towards the imaginary axis, manifesting better capacitive behavior. Meanwhile a semicircle at high frequency is not detected for the two types of electrodes, which can be ascribed to the low interfacial charge-transfer resistance [45].

The equivalent series resistance (ESR) is determined by the intercept at the x-axis of the EIS plot and it is related to the electrolyte solution resistance, the interfacial contact resistance between current collectors and active materials, and the intrinsic resistance of active materials. It is seen from the inset of Fig. 5(c) that the lCNT-GO/PPy electrodes have smaller ESR than the sCNT-GO/PPy electrodes. Moreover, “knee frequency” is another

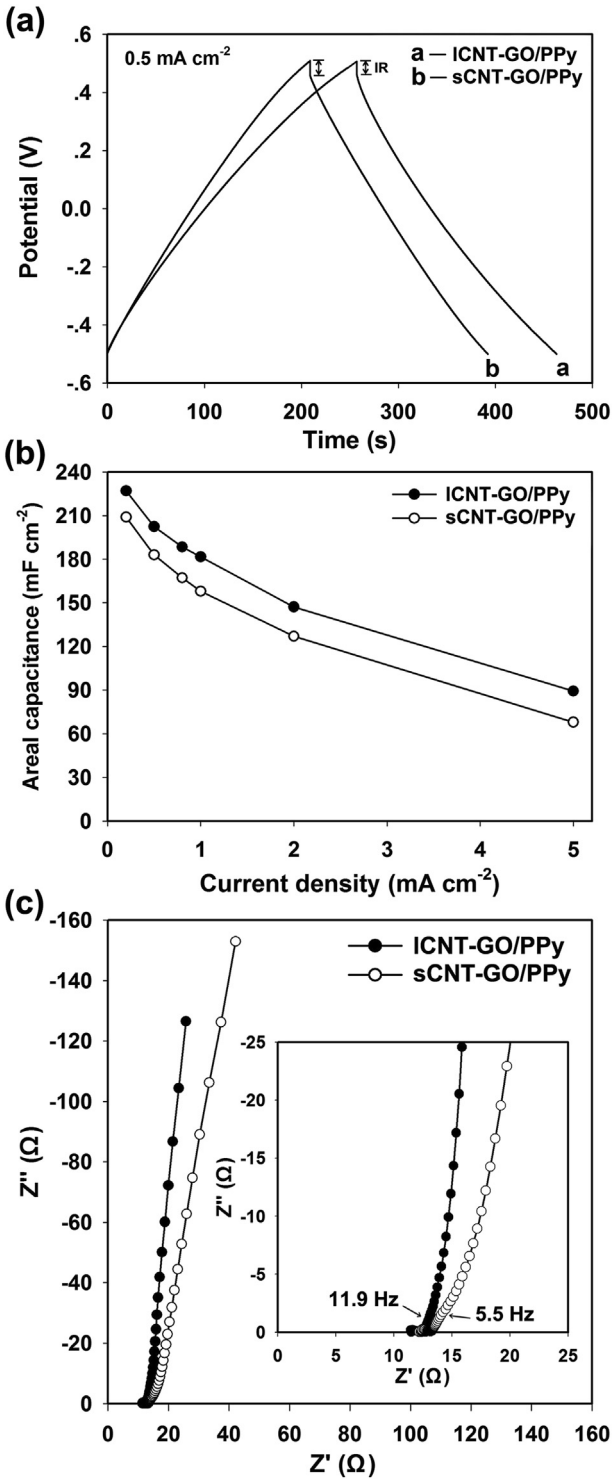

Fig. 5. GCD curves at the current density of 0.5 mA cm^{-2} (a), areal capacitance vs. GCD current density (b), and EIS complex plane plots (c) of sCNT-GO/PPy and lCNT-GO/PPy composite electrodes. The inset in (c) is the EIS in the high-frequency region.

important parameter that can be obtained at the low frequency. It is defined as the maximum frequency at which predominant capacitive behavior is maintained, and a higher knee frequency represents faster charge transfer rates and lower diffusion impedance [46]. The lCNT-GO/PPy electrodes show a higher knee frequency (11.9 Hz; see the inset of Fig. 5(c)) with respect to the sCNT-GO/PPy

electrodes (5.5 Hz). The EIS tests further demonstrate that the lCNT-GO/PPy electrodes have superior properties for charge transfer and ion diffusion of electrolyte, consequently displaying ideal capacitive behavior.

As observed from the morphology characterizations by SEM and TEM, the long CNT doped lCNT-GO/PPy electrodes show superior electrochemical performances with respect to short CNT doped sCNT-GO/PPy electrodes. This is ascribed to the fact that the lCNT-GO/PPy composites have loose and porous features as the abundant, anionic CNTs introduced, which make the composites less compact. These long CNTs penetrate within the composites, forming an interconnected, conductive nano-network that can effectively improve the charge transport.

3.3. Assembled supercapacitor device

To demonstrate the feasibility of the composite electrodes for use as flexible supercapacitor devices, a flexible solid-state supercapacitor with sandwich structure was assembled. It is composed of two symmetric lCNT-GO/PPy composite coated CNFs as electrodes and PVA-H_3PO_4 gel as the solid electrolyte. Fig. 6 shows the electrochemical properties of the assembled flexible solid-state supercapacitor. We can see from Fig. 6(a) that all CV curves maintain the rectangular shape at varying scan rates and the current increases obviously with the scan rates, manifesting the highly capacitive nature.

The supercapacitor device delivers a high specific capacitance of 70.0 mF cm^{-2} at 10 mV s^{-1}, which follows a smooth decline with the increase of CV scan rates (Fig. 6(b)), indicative of superior rate capability. Likewise, the GCD curves (Fig. 6(c)) at varying current densities show symmetric, triangular shape and almost linear potential-time relationship, achieving a high specific capacitance of 72.3 mF cm^{-2} at 0.5 mA cm^{-2}. This value is higher than or comparable with other reported solid-state supercapacitors based on graphene/polyaniline composite (23 mF cm^{-2} at 0.1 mA cm^{-2}) [47], reduced GO film (33.8 mF cm^{-2} at 1 mA cm^{-2}) [48], cellulose nanofibers/[PANI-PEDOT] (4.22 mF cm^{-2} at 0.0043 mA cm^{-2}) [49], and graphite nanosheets/PANI (77.8 mF cm^{-2} at 0.1 mA cm^{-2}) [50]. Moreover, the specific capacitance obtained from GCD tests (Fig. 6(d)) also shows the relatively smooth decline with the increase of current density, maintaining 62% of the initial capacitance when the current density increases by as much as 20 times (45.0 mF cm^{-2} at 10 mA cm^{-2}), which demonstrates that the flexible solid-state supercapacitor device assembled has ideal electrochemical capacitive properties.

The areal specific energy density and power density of this device can be calculated by Eqs. (3) and (4) [21,42], respectively:

$$E = \frac{1}{2} C_S \Delta V^2 \tag{3}$$

$$P = \frac{E}{t} \tag{4}$$

where E is the areal specific energy density in Wh cm^{-2}, P the areal specific power density in W cm^{-2}, C_S the areal specific capacitance of the device in F cm^{-2} obtained from the GCD curves, ΔV the potential window subtracting IR drop in V, and t the discharge time in h. The device shows high power-energy character, as observed from the Ragone plot (Fig. 7(a)). It achieves the highest power density of 3.7 mW cm^{-2} and the maximum energy density of 6.3 μWh cm^{-2}, which are higher than those of recently reported CPs composites

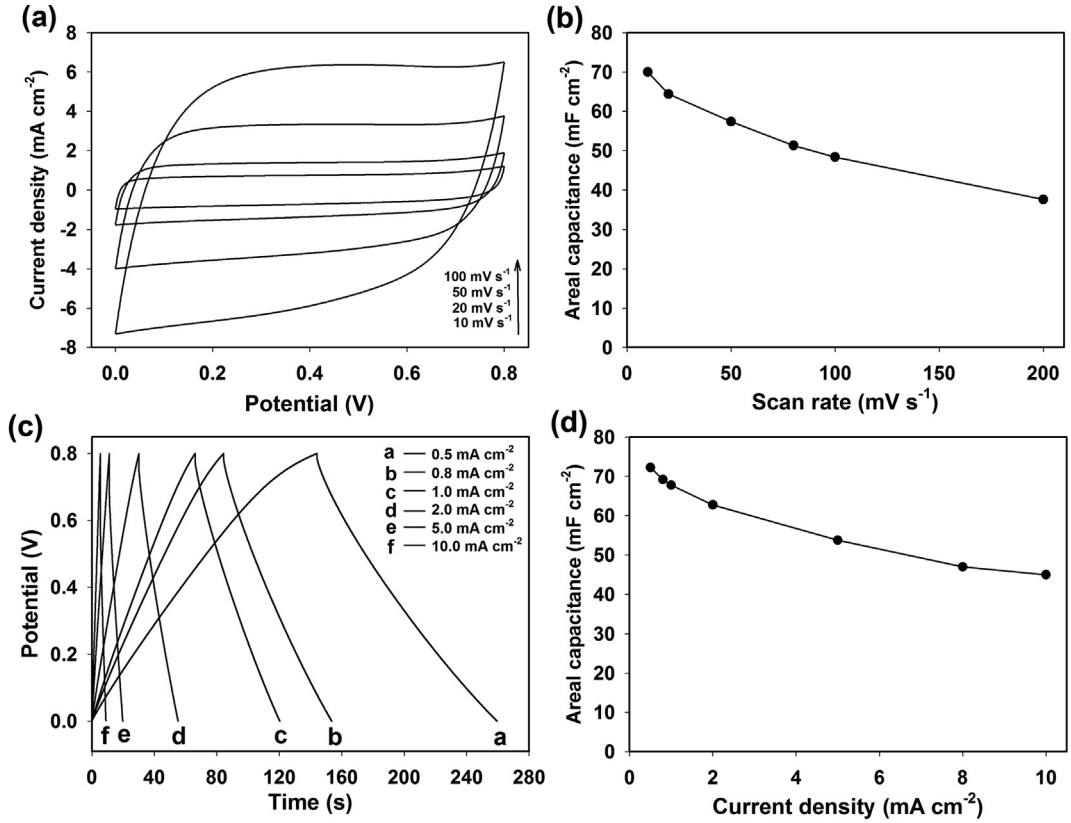

Fig. 6. CV curves at different scan rates (a), areal capacitance *vs.* CV scan rate (b), GCD curves at varying current densities (c), and areal capacitance vs. GCD current density (d) of the flexible solid-state supercapacitor assembled by two symmetric lCNT-GO/PPy composite electrodes with PVA/H_3PO_4 gel as the solid electrolyte. The areal specific capacitance of the device based on the CV and GCD curves is calculated according to the Eq. (1) and Eq. (2), multiplied by 1/2, respectively.

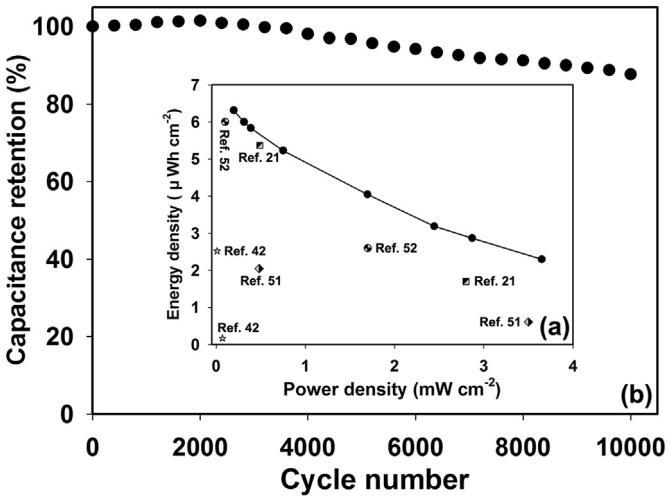

Fig. 7. (a) Ragone plots of the flexible solid-state supercapacitor assembled by two identical lCNT-GO/PPy composite electrodes and the values of recently reported CPs composites based supercapacitors for comparison. (b) The relationship between specific capacitance retention rate and cycle number with 50 mV s^{-1} CV scan for this supercapacitor.

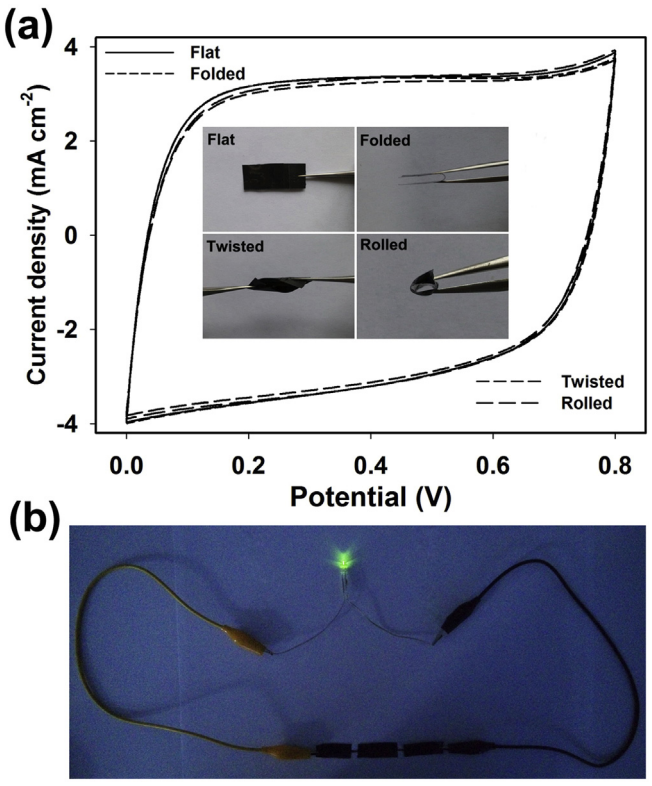

Fig. 8. CV curves at 50 mV s^{-1} (a) for the flexible solid-state supercapacitor under four different states and photograph of a green light-emitting diode (LED) powered by a three-supercapacitor tandem device (b). The inset in (a) is optical photographs of the supercapacitor with four states: flat, folded, twisted, and rolled. (For interpretation of the references to colour in this figure legend, the reader is referred to the web version of this article.)

based supercapacitors, including GO/PPy [21], graphite oxide/PANI [42], carbon paper-PPy [51], and GO/PEDOT [52].

It is well known that high cycle stability is crucial for supercapacitors in practical applications. Fig. 7(b) presents the test result for cycle stability of the device, which underwent 5000 C<superscript></superscript> V<superscript></superscript> cycles at the scan rate of 50 mV s^{-1}. The capacitance of the supercapacitor increases at the first 2000 cycles due to the self-activation process [53] and then gradually decreases at the subsequent cycles, maintaining 87.7% of the initial capacitance after 10000 cycles, suggesting its superior cycle stability.

For applications of the flexible integrated electronic devices, supercapacitors as power sources should have high flexibility without deteriorating the device performance. It can be seen from Fig. 8 (a) that the as-prepared supercapacitor shows high flexibility, which endured the folded, twisted, and rolled states. Its construction was not destroyed. Importantly, the electrochemical property of the device retained nearly unchanged at these states. Meanwhile, the device features lightweight and thinness. The weight and thickness of the whole device (including two identical electrodes, electrolyte, and separator) are only around 115 μm and 26.4 mg, respectively. The volumetric specific capacitance of the device can be calculated using Eq. (2), multiplying by 1/2, in which the area (S) is replaced by volume (V). The device exhibits the volumetric specific capacitance of 6.3 F cm^{-3} at 0.043 A cm^{-3}, which is maintained for 4.1 F/cm^3 at 0.7 A/cm^3. These values are higher than those of the previously reported solid-state supercapacitors, such as graphene based supercapacitors of 0.45 F cm^{-3} [54], H–TiO_2 based asymmetric supercapacitors of 0.7 F cm^{-3} [55], carbon fiber/MnO_2 based supercapacitors of 2.5 F/cm^{-3} [56], and WO_{3-x}/MoO_{3-x} based asymmetric supercapacitors of 3.8 F cm^{-3} [57]. These features make the design of compact and light devices possible. Furthermore, as shown in Fig. 8(b), a three-supercapacitor tandem device was fabricated to lighten a LED. This observation should stimulate the practical uses as the power sources in flexible and lightweight electronic equipments.

4. Conclusions

We have fabricated flexible ternary electrodes using the CNT-GO/PPy composite coated CNFs by electrochemical polymerization. The introduction of CNTs with high conductivity in the composites significantly improves the capacitive performances of the GO/PPy electrodes. The long CNTs doped lCNT-GO/PPy electrodes show superior electrochemical performances as compared to the short CNTs doped sCNT-GO/PPy electrodes. Furthermore, two symmetric lCNT-GO/PPy electrodes are assembled as a high-performance, highly flexible solid-state supercapacitor device. The device features lightweight, thinness, and high flexibility. It is demonstrated to deliver a high specific capacitance and superior cycle stability. This highly flexible supercapacitor device is very promising for uses in wearable devices, flexible electronics, and roll-up display.

Acknowledgements

This work was supported by the National Natural Science Foundation of China (21573138), the Natural Science Foundation of Shanxi Province (2015021079), China Postdoctoral Science Foundation (2015M571283), and the Scientific Research Start-up Funds of Shanxi University (203533801002).

References

[1] M. Acerce, D. Voiry, M. Chhowalla, Metallic 1T phase MoS_2 nanosheets as supercapacitor electrode materials, Nat. Nanotechnol. 10 (2015) 313–318.
[2] L.B. Liu, Y. Yu, C. Yan, K. Li, Z.J. Zheng, Wearable energy-dense and power-dense supercapacitor yarns enabled by scalable graphene-metallic textile composite electrodes, Nat. Commun. 6 (2015) 7260.
[3] J. Xu, D.X. Wang, L.L. Fan, Y. Yuan, W. Wei, R.N. Liu, S.J. Gu, W.L. Xu, Fabric electrodes coated with polypyrrole nanorods for flexible supercapacitor

application prepared via a reactive self-degraded template, Org. Electron. 26 (2015) 292–299.
[4] Z.Y. Xiong, C.L. Liao, W.H. Han, X.G. Wang, Mechanically tough large-area hierarchical porous graphene films for high-performance flexible supercapacitor applications, Adv. Mater. 27 (2015) 4469–4475.
[5] Y.D. Zhang, B.P. Lin, Y. Sun, P. Han, J.C. Wang, X.J. Ding, X.Q. Zhang, H. Yang, MoO_2@Cu@C composites prepared by using Polyoxometalates@Metal-Organic Frameworks as template for all-solid-state flexible supercapacitor, Electrochim. Acta 188 (2016) 490.
[6] S.H. Lee, J.S. Sohn, S.B. Kulkarni, U.M. Patil, S.C. Jun, J.H. Kim, Modified physicochemical properties and supercapacitive performance via DMSO inducement to PEDOT: PSS active layer, Org. Electron. 15 (2014) 3423–3430.
[7] Q. Chen, Y. Zhao, X.K. Huang, N. Chen, L.T. Qu, Three-dimensional graphitic carbon nitride functionalized graphene-based high-performance supercapacitors, J. Mater. Chem. A 3 (2015) 6761–6766.
[8] S.Y. Wang, L. Ma, M.Y. Gan, S.N. Fu, W.Q. Dai, T. Zhou, X.W. Sun, H.H. Wang, H.N. Wang, Free-standing 3D graphene/polyaniline composite film electrodes for high-performance supercapacitors, J. Power Sources 299 (2015) 347–355.
[9] X.X. Pan, X.M. Chen, Y. Li, Z.N. Yu, Facile synthesis of Co_3O_4 nanosheets electrode with ultrahigh specific capacitance for electrochemical supercapacitors, Electrochim. Acta 182 (2015) 1101–1106.
[10] X.H. Lu, M.H. Yu, G.M. Wang, Y.X. Tong, Y. Li, Flexible solid-state supercapacitors: design, fabrication and applications, Energy Environ. Sci. 7 (2014) 2160–2181.
[11] P. Zhang, Z.M. Liu, Y.P. Liu, H.B. Fan, Y.Q. Jiao, B.M. Chen, Titanium Dioxide@Polyaniline core-shell nanowires as high-performance and stable electrodes for flexible solid-state supercapacitors, Electrochim. Acta 184 (2015) 1–7.
[12] D.Z. Kong, W.N. Ren, C.W. Cheng, Y. Wang, Z.X. Huang, H.Y. Yang, Three-dimensional $NiCo_2O_4$@Polypyrrole coaxial nanowire arrays on carbon textiles for high-performance flexible asymmetric solid-state supercapacitor, ACS Appl. Mater. Interfaces 7 (2015) 21334–21346.
[13] Q.Y. Liao, N. Li, S.X. Jin, G.W. Yang, C.X. Wang, All-solid-state symmetric supercapacitor based on Co_3O_4 nanoparticles on vertically aligned graphene, ACS Nano 9 (2015) 5310–5317.
[14] R. Liu, S.B. Lee, MnO_2/Poly(3,4-ethylenedioxythiophene) coaxial nanowires by one-step coelectrodeposition for electrochemical energy storage, J. Am. Chem. Soc. 130 (2008) 2942–2943.
[15] W. Zhou, G. Han, Y. Xiao, Y. Chang, W. Yuan, Y. Li, C. Liu, Y. Zhang, Polypyrrole doped with dodecyl benzene sulfonate electrodeposited on carbon fibers for flexible capacitors with high-performance, Electrochim. Acta 176 (2015) 594–603.
[16] H.H. Zhou, G.Y. Han, Y.Z. Chang, D.Y. Fu, Y.M. Xiao, Highly stable multi-wall carbon nanotubes@poly(3,4-ethylenedioxythiophene)/poly(styrene sulfonate) core-shell composites with three-dimensional porous nano-network for electrochemical capacitors, J. Power Sources 274 (2015) 229–236.
[17] A. Osterholm, T. Lindfors, J. Kauppila, P. Damlin, C. Kvarnstrom, Electrochemical incorporation of graphene oxide into conducting polymer films, Electrochim. Acta 83 (2012) 463–470.
[18] J. Li, H.Q. Xie, Y. Li, Fabrication of graphene oxide/polypyrrole nanowire composite for high performance supercapacitor electrodes, J. Power Sources 241 (2013) 388–395.
[19] J.Y. Cao, Y.M. Wang, J.C. Chen, X.H. Li, F.C. Walsh, J.H. Ouyang, D.C. Jia, Y. Zhou, Three-dimensional graphene oxide/polypyrrole composite electrodes fabricated by one-step electrodeposition for high performance supercapacitors, J. Mater. Chem. A 3 (2015) 14445–14457.
[20] W.L. Wu, Y.F. Li, G.H. Zhao, L.Q. Yang, D. Pan, Aldehyde-poly(ethylene glycol) modified graphene oxide/conducting polymers composite as high-performance electrochemical supercapacitors, J. Mater. Chem. A 2 (2014) 18058–18069.
[21] H.H. Zhou, G.Y. Han, Y.M. Xiao, Y.Z. Chang, H.J. Zhai, Facile preparation of polypyrrole/graphene oxide nanocomposites with large areal capacitance using electrochemical codeposition for supercapacitors, J. Power Sources 263 (2014) 259–267.
[22] S. Lehtimaki, M. Suominen, P. Damlin, S. Tuukkanen, C. Kvarnstrom, D. Lupo, Preparation of supercapacitors on flexible substrates with electrodeposited PEDOT/graphene composites, ACS Appl. Mater. Interfaces 7 (2015) 22137–22147.
[23] T. Lindfors, A. Osterholm, J. Kauppila, M. Pesonen, Electrochemical reduction of graphene oxide in electrically conducting poly(3,4-ethylenedioxythiophene) composite films, Electrochim. Acta 110 (2013) 428–436.
[24] T. Lindfors, R.M. Latonen, Improved charging/discharging behavior of electropolymerized nanostructured composite films of polyaniline and electrochemically reduced graphene oxide, Carbon 69 (2014) 122–131.
[25] J. Xu, D.X. Wang, Y. Yuan, W. Wei, L.L. Duan, L.X. Wang, H.F. Bao, W.L. Xu, Polypyrrole/reduced graphene oxide coated fabric electrodes for supercapacitor application, Org. Electron. 24 (2015) 153–159.
[26] H.H. Chang, C.K. Chang, Y.C. Tsai, C.S. Liao, Electrochemically synthesized graphene/polypyrrole composites and their use in supercapacitor, Carbon 50 (2012) 2331–2336.
[27] Y.L. Chen, L.H. Du, P.H. Yang, P. Sun, X. Yu, W.J. Mai, Significantly enhanced robustness and electrochemical performance of flexible carbon nanotube-based supercapacitors by electrodepositing polypyrrole, J. Power Sources 287 (2015) 68–74.
[28] C. Li, H. Bai, G.Q. Shi, Conducting polymer nanomaterials: electrosynthesis and applications, Chem. Soc. Rev. 38 (2009) 2397–2409.
[29] Y. Liu, B. Weng, J.M. Razal, Q. Xu, C. Zhao, Y. Hou, S. Seyedin, R. Jalili, G.G. Wallace, J. Chen, High-performance flexible all-solid-state supercapacitor from large free-standing graphene-PEDOT/PSS films, Sci. Rep. 5 (2015) 17045.
[30] S. Zeng, H. Chen, F. Cai, Y. Kang, M. Chen, Q. Li, Electrochemical fabrication of carbon nanotube/polyaniline hydrogel film for all-solid-state flexible supercapacitor with high areal capacitance, J. Mater. Chem. A 3 (2015) 23864–23870.
[31] W.S. Hummers, R.E. Offeman, Preparation of graphitic oxide, J. Am. Chem. Soc. 80 (1958) 1339.
[32] Y.X. Xu, H. Bai, G.W. Lu, C. Li, G.Q. Shi, Flexible graphene films via the filtration of water-soluble noncovalent functionalized graphene sheets, J. Am. Chem. Soc. 130 (2008) 5856–5857.
[33] C.Z. Zhu, J.F. Zhai, D. Wen, S.J. Dong, Graphene oxide/polypyrrole nanocomposites: one-step electrochemical doping, coating and synergistic effect for energy storage, J. Mater. Chem. 22 (2012) 6300–6306.
[34] S. Bhandari, M. Deepa, A.K. Srivastava, A.G. Joshi, R. Kant, Poly(3,4-ethylenedioxythiophene)-Multiwalled carbon nanotube composite films: structure-directed amplified electrochromic response and improved redox activity, J. Phys. Chem. B 113 (2009) 9416–9428.
[35] S. Konwer, R. Boruah, S.K. Dolui, Studies on conducting polypyrrole/graphene oxide composites as supercapacitor electrode, J. Electron. Mater. 40 (2011) 2248–2255.
[36] T.M. Wu, S.H. Lin, Synthesis, characterization, and electrical properties of polypyrrole/multiwalled carbon nanotube composites, J. Polym. Sci. Pol. Chem. 44 (2006) 6449–6457.
[37] K. V, E. Frackowiak, F. Beguin, Determination of the specific capacitance of conducting polymer/nanotubes composite electrodes using different cell configurations, Electrochim. Acta 50 (2005) 2499–2506.
[38] Y.Y. Horng, Y.C. Lu, Y.K. Hsu, C.C. Chen, L.C. Chen, K.H. Chen, Flexible supercapacitor based on polyaniline nanowires/carbon cloth with both high gravimetric and area-normalized capacitance, J. Power Sources 195 (2010) 4418–4422.
[39] G.M. Wang, H.Y. Wang, X.H. Lu, Y.C. Ling, M.H. Yu, T. Zhai, Y.X. Tong, Y. Li, Solid-state supercapacitor based on activated carbon cloths exhibits excellent rate capability, Adv. Mater. 26 (2014) 2676–2682.
[40] C. Huang, N.P. Young, P.S. Grant, Spray processing of TiO_2 nanoparticle/ionomer coatings on carbon nanotube scaffolds for solid-state supercapacitors, J. Mater. Chem. A 2 (2014) 11022–11028.
[41] M.H. Yu, Y.X. Zeng, C. Zhang, X.H. Lu, C.H. Zeng, C.Z. Yao, Y.Y. Yang, Y.X. Tong, Titanium dioxide@polypyrrole core-shell nanowires for all solid-state flexible supercapacitors, Nanoscale 5 (2013) 10806–10810.
[42] H.G. Wei, J.H. Zhu, S.J. Wu, S.Y. Wei, Z.H. Guo, Electrochromic polyaniline/graphite oxide nanocomposites with endured electrochemical energy storage, Polymer 54 (2013) 1820–1831.
[43] R.Z. Li, X. Ren, F. Zhang, C. Du, J.P. Liu, Synthesis of Fe_3O_4@SnO_2 core-shell nanorod film and its application as a thin-film supercapacitor electrode, Chem. Commun. 48 (2012) 5010–5012.
[44] Q.Q. Zhou, Y.R. Li, L. Huang, C. Li, G.Q. Shi, Three-dimensional porous graphene/polyaniline composites for high-rate electrochemical capacitors, J. Mater. Chem. A 2 (2014) 17489–17494.
[45] Y.Q. Han, B. Ding, H. Tong, X.G. Zhang, Capacitance properties of graphite oxide/poly(3,4-ethylene dioxythiophene) composites, J. Appl. Polym. Sci. 121 (2011) 892–898.
[46] Y. Song, J.L. Xu, X.X. Liu, Electrochemical anchoring of dual doping polypyrrole on graphene sheets partially exfoliated from graphite foil for high-performance supercapacitor electrode, J. Power Sources 249 (2014) 48–58.
[47] X.B. Zang, X. Li, M. Zhu, X.M. Li, Z. Zhen, Y.J. He, K.L. Wang, J.Q. Wei, F.Y. Kang, H.W. Zhu, Graphene/polyaniline woven fabric composite films as flexible supercapacitor electrodes, Nanoscale 7 (2015) 7318–7322.
[48] U.N. Maiti, J. Lim, K.E. Lee, W.J. Lee, S.O. Kim, Three-dimensional shape engineered, interfacial gelation of reduced graphene oxide for high rate, large capacity supercapacitors, Adv. Mater. 26 (2014) 615–619.
[49] X. Wang, K.Z. Gao, Z.Q. Shao, X.Q. Peng, X. Wu, F.J. Wang, Layer-by-Layer assembled hybrid multilayer thin film electrodes based on transparent cellulose nanofibers paper for flexible Supercapacitors applications, J. Power Sources 249 (2014) 148–155.
[50] B. Yao, L.Y. Yuan, X. Xiao, J. Zhang, Y.Y. Qi, J. Zhou, J. Zhou, B. Hu, W. Chen, Paper-based solid-state supercapacitors with pencil-drawing graphite/polyaniline networks hybrid electrodes, Nano Energy 2 (2013) 1071–1078.
[51] H.G. Wei, Y.R. Wang, J. Guo, X.R. Yan, R. Connor, X. Zhang, N.Z. Shen, B.L. Weeks, X.H. Huang, S.Y. Wei, Z.H. Guo, Electropolymerized polypyrrole nanocoatings on carbon paper for electrochemical energy storage, ChemElectroChem 2 (2015) 119–126.
[52] H.H. Zhou, H.J. Zhai, G.Y. Han, Adjust the electrochemical performances of graphene oxide nanosheets-loaded poly(3,4-ethylenedioxythiophene) composites for supercapacitors with ultralong cycle life, J. Mater. Sci. Mater. Electron. 27 (2016) 2773–2782.
[53] L.Y. Yuan, B. Yao, B. Hu, K.F. Huo, W. Chen, J. Zhou, Polypyrrole-coated paper for flexible solid-state energy storage, Energy Environ. Sci. 6 (2013) 470–476.
[54] M.F. El-Kady, V. Strong, S. Dubin, R.B. Kaner, Laser scribing of high-performance and flexible graphene-based electrochemical capacitors, Science 335 (2012) 1326–1330.
[55] X.H. Lu, M.H. Yu, G.M. Wang, T. Zhai, S.L. Xie, Y.C. Ling, Y.X. Tong, Y. Li, H-TiO_2@MnO_2//H-TiO_2@C core-shell nanowires for high performance and

flexible asymmetric supercapacitors, Adv. Mater. 25 (2013) 267–272.
[56] X. Xiao, T.Q. Li, P.H. Yang, Y. Gao, H.Y. Jin, W.J. Ni, W.H. Zhan, X.H. Zhang, Y.Z. Cao, J.W. Zhong, L. Gong, W.C. Yen, W.J. Mai, J. Chen, K.F. Huo, Y.L. Chueh, Z.L. Wang, J. Zhou, Fiber-based all-solid-state flexible supercapacitors for self-powered systems, ACS Nano 6 (2012) 9200–9206.
[57] X. Xiao, T.Q. Li, Z.H. Peng, H.Y. Jin, Q.Z. Zhong, Q.Y. Hu, B. Yao, Q.P. Luo, C.F. Zhang, L. Gong, J. Chen, Y. Gogotsi, J. Zhou, Freestanding functionalized carbon nanotube-based electrode for solid-state asymmetric supercapacitors, Nano Energy 6 (2014) 1–9.